Comparison between Supercritical Combustion Modelling for LO2-CH4 Rocket Engines at 15MPa using Real and Ideal gas properties

A.Minotti and C. Bruno*+*

Department of Mechanics and Aeronautics, University of Rome "La Sapienza", Via Eudossiana 18, 00184, Rome, Italy

** +390644585272, angelominotti@inwind.it*

**+ +390644585280, Claudio.Bruno@uniroma1.it*

OVERVIEW

In this work mixing and combustion processes in LRE between ideal and real gases in supercritical regime are studied. Two FANS simulations of a LO_2/CH_4 coaxial reacting jet are presented. All are performed with supercritical methane and supercritical oxygen jet injection conditions and are carried on using first real gas properties and then ideal gas properties. Real gas properties are predicted using particular fitting polynomials, a single reaction is assumed and combustion is modeled by the Eddy Dissipation concept. Simulations show how real and ideal gas properties predict different maximum temperature and pressure and that particular attention must be taken to the potential core length design parameter.

1. INTRODUCTION

In [1] the differences between real and ideal gas behaviour have been analyzed and thermophysical properties have been quantified. That work has shown that assuming ideal gas behaviour in transcritical conditions leads to large errors. Therefore, accurate real gas properties modeling is mandatory to simulate Liquid Rocket Engines (LRE) in sub-trans and supercritical conditions. These properties have been described by means of polynomials fits [1] based on:

1. experimental data (from NIST tables) and data obtained with the Lee-Kesler [2] equation of state (EOS), for what concerns density and isobaric heat capacity;
2. experimental data (from NIST tables) and data obtained with the Chung et al. method [3], for what concerns viscosity and thermal conductivity.

These polynomial fits have been validated by simulating and comparing the results of N_2 injection at supercritical temperature in a N_2 atmosphere chamber [4], and N_2 injection at subcritical conditions in a N_2 atmosphere chamber [4,5]. After validation, two LO_2/CH_4 non-reacting coaxial jet simulations, at sub and supercritical conditions, have been carried on and studied [1] and the results have been compared with Villermaux prediction theory [6,7] and with those in [8]. The two LO_2/CH_4 simulations included are a reacting coaxial injection of LO_2-CH_4, with supercritical CH_4 injection and supercritical O_2 injection carried on with, at first, ideal and, later, real gas properties.

The purpose of this study is to investigate the mixing (length of the potential core) and combustion processes inside a combustion chamber in order to have useful design indications.

In literature there are other simulations of subcritical and supercritical problems: by Chehroudi [9,10], Mayer and Tamura [11,12,13,14], and J. Oefelein and V. Yang [15,16,17,18,19] and N.O'Kongo, K. Harstad and J.Bellan [20,21].

Table 1 reports the critical conditions of the species analyzed in this study.

	T_c [K]	P_c[atm]
O_2	154.6	49.8
CO_2	304.2	72.8
H_2O	647.3	217.6
CH_4	190.4	46

Table 1: Critical properties of species assumed of interest to LRE

2. OXYGEN/METHANE COAXIAL JET REACTING SIMUALTIONS

Two reacting simulations of an axial symmetry reacting LO_2/CH_4 coaxial jets are presented. All use the same geometry (see fig. 1), computational mesh (32600 cells) and boundary conditions: inlet mass flow imposed, constant temperature on the walls, adiabatic heat flux on the post tip, slip wall at the outer boundary and constant pressure at the outlet.

Simulations reproduce a supercritical CH_4 jet that reacts with a supercritical O_2, using real gas and ideal gas properties. Both use time dependent FANS equation with a k-ε turbulence model and the simulations reach stationary conditions. One single global reaction is assumed:

(1) $$CH_4+2O_2 \rightarrow CO_2+ 2H_2O$$

The subsequent over-estimated maximum temperature is managed by a modified methane formation enthalpy: $\Delta H'_{fCH4}=-1.3\times10^8$ [J/kgmol] [22].
The source term *($R_{i,r}$)* of the *i*-specie production is modelled by means of an Eddy-Dissipation model [23,24,25,26,27,28]:

(2) $$R_{i,r} = \nu'_{i,r} M_{w,i} A \rho \frac{\varepsilon}{k} \min_{\Re}\left(\frac{Y_{\Re}}{\nu'_{i,r} M_{w,\Re}}\right)$$

where
$Y_{\Re}\equiv$ mass fraction of the reactant $\Re$;
A ≡ empirical constant, 4.0;
$\frac{\varepsilon}{k}\equiv$ reverse of turbulent time scale;
$\nu'_{i,r}\equiv$ stechiometric coefficient of the *i*-species in reaction *r*;
The key point of this model is that chemical times are much shorter than those of turbulence and that thus each reaction velocity is controlled by the rate of turbulent mixing.

2.1. Supercritical CH_4 reacting with supercritical O_2 using real gas properties

The operating conditions of the case analyzed with real gas properties are reported in Table 2, pressure and temperature are supercritical for both the reactants.

	O_2	CH_4
Pressure [MPa]	15	15
Temperature [K]	300	300
Mass flow [kg/s]	0.386	0.114
Velocity [m/s]	49.4	31.8
Molecular Viscosity [kg/m-s]	2.74×10^{-5}	1.23×10^{-5}
Density [kg/m^3]	200	117
Reynolds number	2524000	302000
Isobaric Specific Heat [J/kgK]	1166.3	3379.8

Table 2: LO2/CH4 with real gas properties, operating conditions

Results reported below show a steady flow simulation snapshot. Figure 2 shows the axial pressure that is not constant along the axis, with the highest value around 16.5MPa (1.5MPa higher than the exhaust pressure). Figure 3 reports the axial O_2 mass fraction : as in the non reacting simulation [22], the O_2 mass fraction never reaches, along the combustion chamber axis, the reference value defined to estimate the length of the potential core, equal to 0.9 [22] . Figure 4 reports the radial temperature at different axial sections (the maximum temperature is around 3770K) ; figures 5 to 8 show the reactants and products radial mass fraction at different axial sections, respectively fig. 5 for O_2, fig. 6 for CH_4, fig. 7 for CO_2 and fig. 8 for H_2O.

2.2. Supercritical CH_4 reacting with supercritical O_2 using ideal gas properties

This analysis is about the supercritical reacting O_2/CH_4 coaxial injector carried on using ideal gas properties at the same boundary conditions of the previous case : this has been done in order to asses the effect of the compressibility factors $Z\neq1$, which at these operating conditions are equal to $Z_{CH4}=0.8$ and $Z_{O2}=0.9$ [22]. Comparing Table 2 with Table 3 the first differences can be shown : ideal gas properties [29,30,31,32] lead to different densities and viscosities, so providing different Oxygen and Methane Reynolds numbers and different inlet velocities.

	O_2	CH_4
Pressure [MPa]	15	15
Temperature [K]	300	300
Mass flow [kg/s]	0.386	0.114
Velocity [m/s]	46.5	38.3
Molecular Viscosity [kg/m-s]	2.06×10^{-5}	1.12×10^{-5}
Density [kg/m^3]	216	108
Reynolds number	3430000	331000
Isobaric Specific Heat [J/kgK]	918.3	2229.1

Table 3: LO2/CH4 with ideal gas properties, operating conditions

The different values shown in the two previous tables are quantified in percentage, (((ideal-real)/ideal)*100), in the following table 4.

	O_2	CH_4
Velocity	6.2 %	16.97 %
Molecular Viscosity	-33 %	9.8 %
Density	7.4 %	-8.3 %
Reynolds number	26.4 %	8.7 %
Isobaric Specific Heat	-27 %	-51 %

Table 4: reactants properties % differences beteween real and ideal behaviour

Is evident that, despite the fact that both the reactants are injected at supercritical conditions, both for temperature

and pressure, differences are not negligible and in fact they lead to the different final results shown below.
The supercritical reacting simulation reaches steady state conditions with ideal properties too. Figure 9 reports the axial pressure ; also in this case pressure is not constant and the maximum value is around 17MPa, 2MPa higher than the exhaust pressure and 0.5MPa higher than corresponding simulation carried on with real gas properties. The potential core, see fig. 10, is longer than the axial combustion chamber extension; the same happens also in the non reacting simulation [22].
The maximum temperature is 4320K, i.e. it's higher by 500K than the maximum temperature obtained with real gas properties : this is due to the reactants different isobaric specific heat behaviours at low temperature, see fig. 16 and fig. 17. Figure 11 shows the radial tempertaure at different axial sectons while figures 12 to 15 show the reactants and products radial mass fractions at different axial sections, i.e. fig. 12 for O_2, fig. 13 for CH_4, fig. 14 for CO_2 and fig. 15 for H_2O. Table 5 shows the comparison between the results obtained with the two methodologies.

	Ideal	**Real**
Non Reacting Potential Core Length [22]	x/d > 15	x/d > 15
Reacting Potential core length	x/d > 15	x/d > 15
Reacting Simulation	Steady State	Steady State
Maximum Temperature	4320K	3770K
Maximum Pressure	16.9MPa	16.4MPa

Table 5: Ideal and real gas properties: results comparison

3. CONCLUSIONS

This study has focused on the mixing and combustion processes differences between ideal and real gas properties of a supercritical LO_2/CH_4 coaxial injector. Purposely calculated polynomials to define real gas properties have been used [1,22]. Compared results are provided in Table 4. Both the methodologies predict pressure as not constant inside the chamber pressure, exactly ideal gas simulations provide a higher chamber pressure than predicted using real gas: this is due to the higher temperature predicted in the "ideal combustion chamber" by the different isobaric specific heat behaviours, fig. 16 and fig. 17. In both cases, combustion provides a length of the potential core longer than the computational domain axial extension. In summing up if ideal gas properties are used, to simulate supercritical real gas conditions, we will overestimate temperature and pressure parameters and both the simulations show that special care must be taken for the length of the combustion chamber design parameter.

4. FIGURES

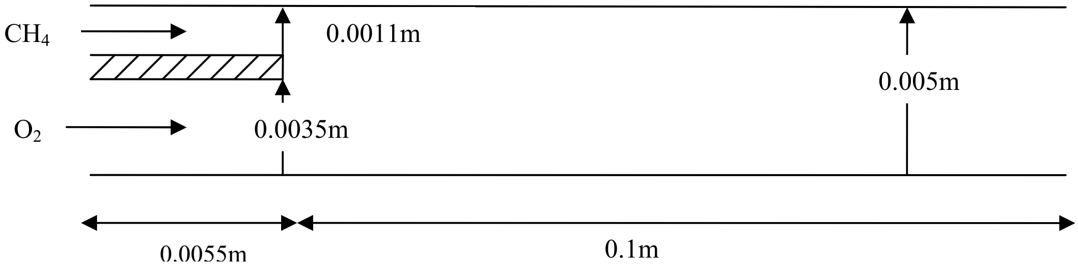

Figure 1: LO_2/CH_4 schematic diagram of the computational domain

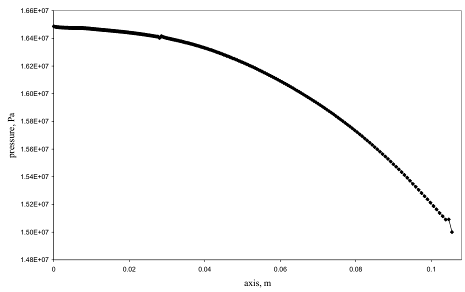

Figure 2: Real gas: axial pressure

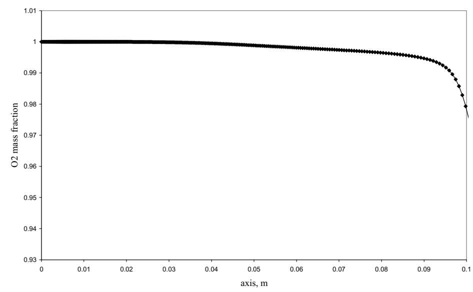

Figure 3: Real gas: O_2 axial mass fraction

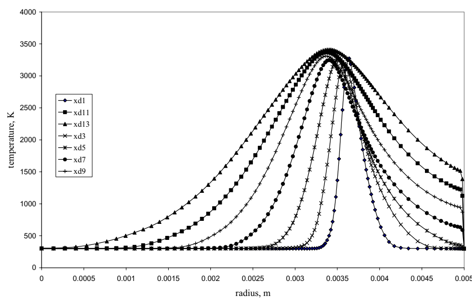

Figure 4: Real gas: radial temperature at different axial sections

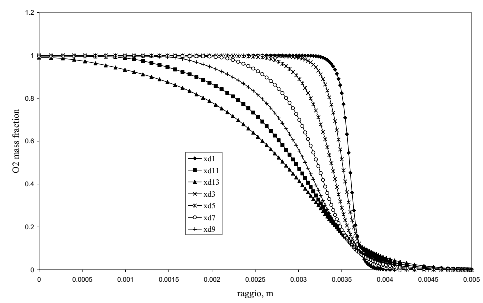

Figure 5: Real gas: O_2 radial mass fraction at different axial sections

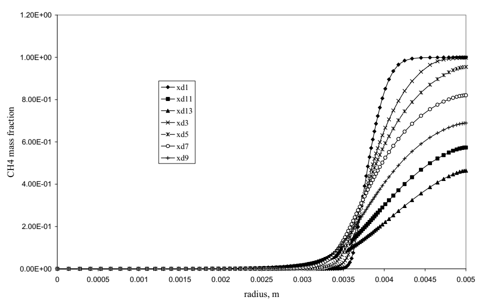

Figure 6: Real gas: CH_4 radial mass fraction at different axial sections

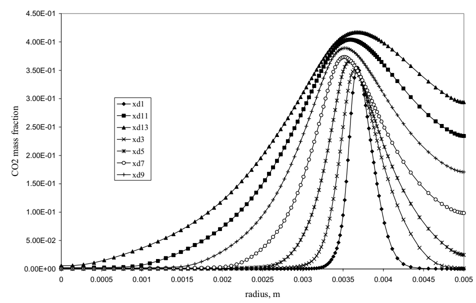

Figure 7: Real gas: CO_2 radial mass fraction at different axial sections

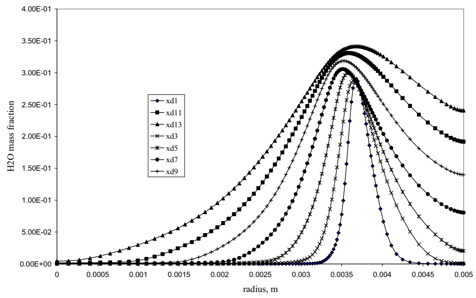

Figure 8: Real gas: H_2O radial mass fraction at different axial sections

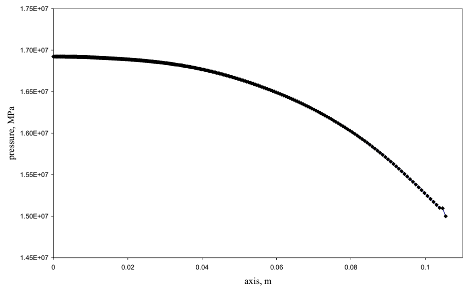

Figure 9: Ideal gas, axial pressure

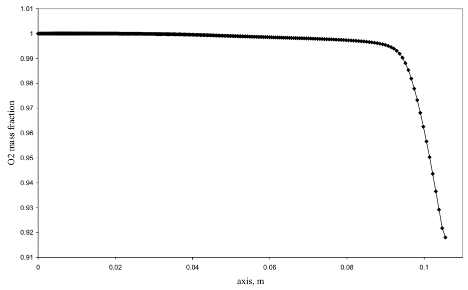

Figure 10: Ideal gas: O_2 axial mass fraction

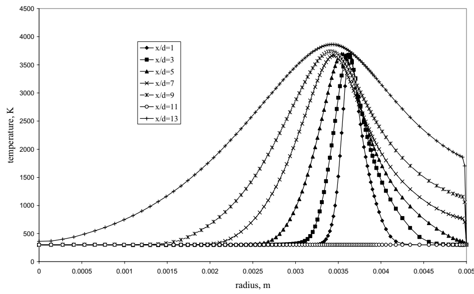

Figure 11: Ideal gas: radial temperature at different axial sections

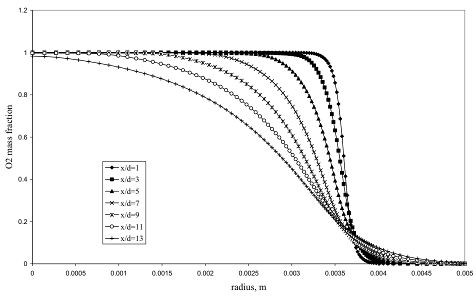

Figure 12: Ideal gas: O_2 radial mass fraction at different axial sections

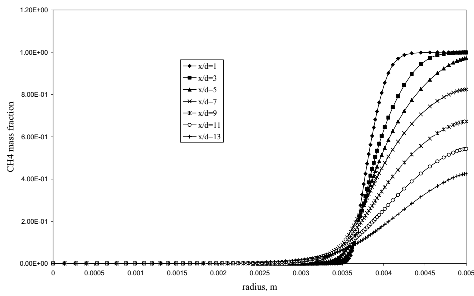

Figure 13: Ideal gas: CH_4 radial mass fraction at different axial sections

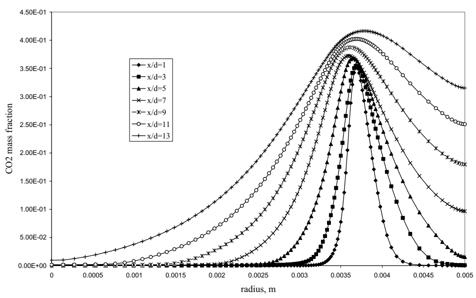

Figure 14: Ideal gas: CO_2 radial mass fraction at different axial sections

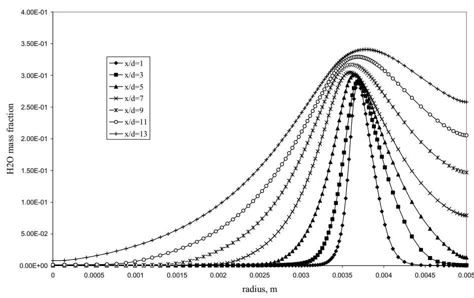

Figure 15: Ideal gas: H_2O radial mass fraction at different axial sections

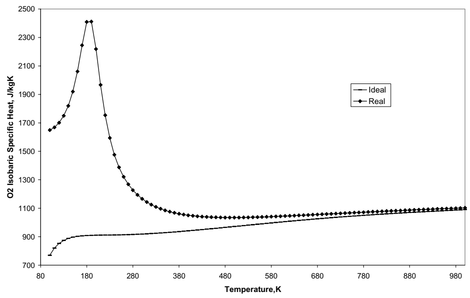

Figure 16: O_2 ideal and real isobaric specific heat, comparison

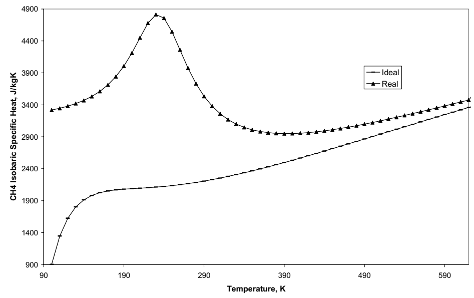

Figure 17: CH_4 ideal and real isobaric specific heat, comparison

REFERENCES

[1] Minotti, A., and Bruno, C., Sub-Trans and Supercritical Properties for LO2-CH4 at 15MPa, accepted by the Journal of Heat Transfer and Thermodynamics, May 2007.
[2] Lee Byung Ik, and Kesler, Micheal G., “A generalized thermodynamic correlation based on three-parameter corresponding states”, AiChE Journal, Vol.21, No.3, pp 510-527, May 1975.
[3] Chung, T.H., Ajlan, M., Lee, L.L., and Starling, K.E., “Generalized multiparameter corresponding state correlation for polyatomic, polar fluid transport properties”, Industrial and Chemical Engineering Research, Vol.27, pp.671-679, 1988.
[4] Mayer, W., Telaar, J., Branana, R., Schneider, G., and Hussong, J., “Characterization of Cryogenic Injection at Supercritical Pressure”, Journal of Propulsion and Power 2003, 0748-4658, Vol. 19 n° 3, pp.342-355.
[5] Haidn, O., J., Proceedings of the 2nd International Workshop on Rocket Combustion Modelling, DLR, Lampoldshausen, ISBN 3-00-008892-X-2001, March 25-27, 2001.
[6] Rehab, H., Villermaux, E., and Hopfinger, E., “Flow Regimes of large velocity ratio coaxial jets”, J. Fluid Mech., Vol. 345, 1998, pp. 357-381.
[7] Villermaux, E., “Mixing and Spray Formation in Coaxial Jets”, Journal of Propulsion and Power, Vol. 14, N 5, 1998, pp. 807-817.
[8] Ierardo, N., and Congiunti, A., “Mixing and combustion in supercritical O_2/CH_4 liquid rocket injectors”, 42nd AIAA meeting, 5-8 January 2004, Reno, AIAA 2004-1163.
[9] Chehroudi, B., Talley, D., and Coy, E., “Initial Growth Rate and Visual Characteristic of a Round Jet into a Sub-Supercritical Environment of Relevance to Rocket, Gas Turbine and Diesel Engines”, AIAA 99-0206, 37th AIAA Aerospace Sciences Meeting and Exhibit, Reno, NV, 11-14 January 1999.
[10] Chehroudi, B., Talley, D., and Coy, E., “Fractal Geometry and Growth Rate Changes of Cryogenic Jets Near the Critical Point”, Atomization and Sprays, 2004, vol 14, part 1, pp 81-91.
[11] Mayer, W. and Tamura, H., “Propellant Injection in a Liquid Oxygen/Gaseous Hydrogen Rocket Engine”, AIAA, Journal of Propulsion and Power, Vol. 12, N 6, 1996, pp 1137-1147.
[12] Mayer, W., Schik, A., Schweitzer, C., and Schaffer, M., “Injection and Mixing Process in High Pressure LO_x/GH_2 Rocket Combustors”, Journal of Propulsion and Power 2000, 0748-4658, vol. 16, n° 5, pp 823-828.
[13] Mayer, W., Schik, A., Vielle, B., Chaveau, C., Goekalp, I., Talley, D., and Woodward, R., “Atomization and Breakup of Cryogenic Propellant Under High Pressure Subcritical and Supercritical Conditions”, Journal of Propulsion and Power, 0748-4658, Vol. 14, N 5, pp 835-842, 1998.
[14] Mayer, W., Ivancic, B., Schik, A., and Hornung, U., “Propellant Atomization in LO_x/GH_2 Rocket Engines”, Journal of Propulsion and Power, 2001, 0748-4658, vol 17, n° 4, pp794-799.
[15] Oefelein, J. and Yang, V., “Simulation and Analysis of Supercritical Multiphase Combustion Processes”, AIAA-1996-2880, Joint Propulsion Conference and Exhibit, 32nd, July 1-3, 1996.
[16] Oefelein, J., Simulation and Analysis of Supercritical Multiphase Combustion Processes at High Pressure, Ph.D. thesis, The Pennsylvania State University, Department of Mechanical Engineering, 1997.
[17] Oefelein, J. and Yang, V., “Modelling High Pressure Mixing and Combustion Processes in Liquid Rocket Engines”, Journal of Propulsion and Power, Vol. 14, N 5, , pp 843-857, 1998. [18] Yang, V., Zong, N., “A numerical study of cryogenic fluid injection and mixing under supercritical conditions”, Physics of Fluids, Vol 16, n 12, pp. 4248-4261, December 2004.
[18] Yang, V., Zong, N., “A numerical study of cryogenic fluid injection and mixing under supercritical conditions”, Combustion Science and Technology,Vol.27, n1-2,pp31-43, 1981.
[19] Yang, V., Zong, N., “Near field flow and flame dynamics of LOx/methane shear coaxial injector under

supercritical conditions”, Proceedings of the Combustion Institute 31,2309-2317, 2007
[20] Bellan, J., “Theory, modelling and analysis of turbulent supercritical mixing”, Combustion Science and Technology, Vol. 178, Numbers 1-3, pp. 253-281, January 2006.
[21] O’Kongo, N., Harstad, K., and Bellan, J., “Direct Numerical Simulation of LOX-H_2 temporal mixing layers under supercritical conditions”, in 2nd International Workshop on Rocket Combustion Modelling, DLR Lampoldshausen.
[22] Minotti, A., “Sub-Trans and Supercritical combustion modelling for LOx-HC propulsion”, PhD Thesis, University of Rome “La Sapienza”, Department of Mechanical and Aeronautical Engineering, 2007.
[23] Giacomazzi, E., “Modelling and simulation of turbulent combustion”, PhD Thesis, University of Rome “La Sapienza”, Department of Mechanical and Aeronautical Engineering, 1999.
[24] Gran, I.R., and Magnussen, B.F., “A numerical study of a Bluff-Body stabilized diffusion flame. Part2. Influence of combustion modelling and finite-rate chemistry”, Combustion Science and Technology, Vol. 119, n 1-6, 1996
[25] Magnussen, B.F., “On the structure of turbulence and a generalized eddy dissipation concept for chemical reaction in turbulent flow”, AIAA, Aerospace Science Meeting, 19th, St. Louis, Mo., Jan. 12-15, 1981, 7p.
[26] Magnussen, B.F., and Hjertager, B.H., “On mathematical modelling of turbulent combustion with special emphasis on soot formation and combustion”, 16th Symp. On Comb., the Combustion Institute, Pittsburg, 1977, pp. 719-729.
[27] Spalding, D.B., “Mixing and chemical reaction in steady confined turbulent flames”, 13th Symp. On Comb., the Combustion Institute, Pittsburgh, pp. 649-657, 1971
[28] Westbrook, C.K, F.L. Dryer, “Simplified Reaction Mechanisms for the Oxidation of Hydrocarbon Fuels and Flames”, Combustion Science and Technology, Vol.27, n 1-2, pp 31-43, 1981.
[29] Gordon, S., McBride, B.J., and Zeleznik, F.J., “Computer program for calculation of complex chemical equilibrium composition and applications, supplement I-Transport Properties”, NASA TM-86885, 1984.
[30] Gordon, S., and McBride, B.J., “Computer program for calculating and fitting thermodynamic functions”, NASA RP-1271, 1992.
[31] Gordon, S., McBride, B.J., and Reno, M.A., “Thermodynamic data for fifty reference elements”, NASA TP-3287, 1993a.
[32] Gordon, S., McBride, B.J., and Reno, M.A., “Coefficients for calculating thermodynamic and transport properties of individual species”, NASA TM-4513, 1993b.